

SiC RECESSION DUE TO SiO₂ SCALE
VOLATILITY UNDER COMBUSTION CONDITIONS.
PART II: THERMODYNAMICS AND GASEOUS DIFFUSION MODEL

Elizabeth J. Opila*¹, James L. Smialek*¹, Raymond C. Robinson[&],
Dennis S. Fox*¹, and Nathan S. Jacobson*¹

*Department of Chemical Engineering
Cleveland State University
Cleveland, OH 44115

IN-77
372 770

#NASA Lewis Research Center
Cleveland, OH 44135

&NYMA, Inc.
Brookpark, OH 44142

Abstract

In combustion environments, volatilization of SiO₂ to Si-O-H(g) species is a critical issue. Available thermochemical data for Si-O-H(g) species were used to calculate boundary layer controlled fluxes from SiO₂. Calculated fluxes were compared to volatilization rates of SiO₂ scales grown on SiC which were measured in Part I of this paper. Calculated volatilization rates were also compared to those measured in synthetic combustion gas furnace tests. Probable vapor species were identified in both fuel-lean and fuel-rich combustion environments based on the observed pressure, temperature and velocity dependencies as well as the magnitude of the volatility rate. Water vapor is responsible for the degradation of SiO₂ in the fuel-lean environment. Silica volatility in fuel-lean combustion environments is attributed primarily to the formation of Si(OH)₄(g) with a small contribution of SiO(OH)₂(g). Reducing gases

such as H_2 and/or CO in combination with water vapor contribute to the degradation of SiO_2 in the fuel-rich environment. The model to describe silica volatility in a fuel-rich combustion environment gave a less satisfactory fit to the observed results. Nevertheless, it was concluded, given the known thermochemical data, that silica volatility in a fuel-rich combustion environment is best described by the formation of $SiO(g)$ at one atmosphere total pressure and the formation of $Si(OH)_4(g)$, $SiO(OH)_2(g)$, and $SiO(OH)(g)$ at higher pressures. Other Si-O-H(g) species, such as $Si_2(OH)_6$, may contribute to the volatility of SiO_2 under fuel-rich conditions, however, complete thermochemical data are unavailable at this time.

Introduction

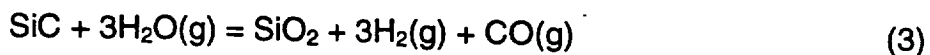
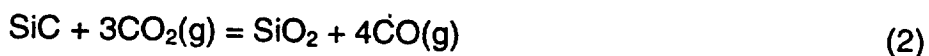
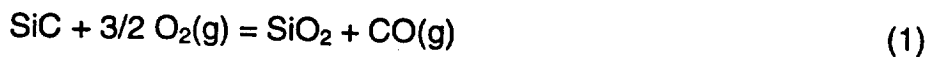
SiC and other Si-based ceramic composites have been proposed for high temperature components in aircraft turbine engines. In Part I of this paper [1], high pressure burner rig (HPBR) testing of CVD SiC in both fuel-lean and fuel-rich environments resulted in linear weight loss and surface recession rates as a result of silica volatility. The objective of this paper is to develop a chemical model for the volatilization of SiO_2 in complex combustion environments which describes the weight loss and surface recession observed for SiC in the HPBR, as well as other furnace tests of SiC in synthetic combustion environments.

The combustion of Jet A Fuel, $CH_{1.9185}$, in air breathing engines gives rise to an environment which always contains N_2 , H_2O , and CO_2 . In fuel-lean environments O_2 is also found. On the other hand, fuel-rich environments

contain H₂ and CO but little O₂. The gas composition of the combustion environment has been discussed in greater detail [2] and is shown in Figure 1 as a function of equivalence ratio, ϕ . Equivalence ratio is a fuel-to-air ratio with total hydrocarbon content normalized to the amount of oxygen. At stoichiometry, $\phi=1$, combustion results in complete consumption of fuel and air. Regardless of fuel-to-air ratio, about 10% of the combustion gas is composed of water vapor. It will be demonstrated in this paper that water vapor is primarily responsible for the degradation of SiC in the combustion environment.

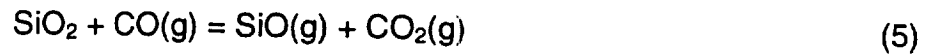
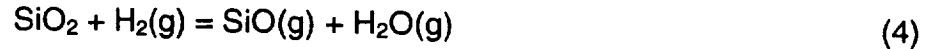
Theory and Literature Review

SiC is thermodynamically unstable in an oxidizing environment and forms an outer scale of SiO₂. Because the SiO₂ forms a protective layer which grows at a slow rate, SiC has been proposed for use in high temperature oxidizing conditions such as combustion environments. In combustion environments containing O₂, CO₂, and H₂O, SiC can oxidize by any or all of the following reactions:

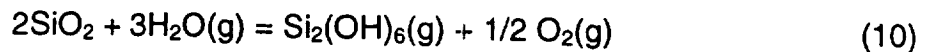
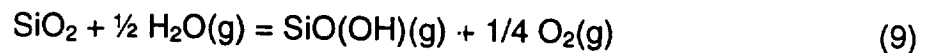
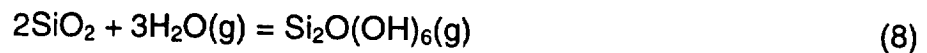


Water vapor has been found to be the primary oxidant based on a comparison of the oxidation rates of SiC in each gas [3].

It has also been shown that in mixed oxidizing/reducing gases [4-6] such as H₂O/H₂ or CO₂/CO mixtures, the silica scale can, in turn, be reduced by one of the following reactions to form volatile SiO(g):



Similarly, in water vapor containing environments the silica scale may react to form volatile hydroxides or oxyhydroxides by one of the following reactions:



Reaction 7 has been observed experimentally by a transpiration method [7] as well as atmospheric sampling mass spectrometry [8]. Reactions 6 and 9 have been observed by Knudsen effusion mass spectrometry [9,10]. Reaction 8 is thought to be important at pressures much higher than those found in turbine engines [11]. Reaction 10 has been described by Krikorian [11], but has not previously been considered important in water vapor containing environments. No experimental data are available for this molecule and estimated data are incomplete.

In conditions, such as combustion environments, where both SiC oxidation and SiO₂ volatilization occur, parabolic kinetics are observed. The oxidation/volatilization kinetics have been modeled by Tedmon [12] for chromia

forming materials and for SiC by Opila & Hann [13]. Paralinear kinetics, expressed in terms of specific weight change, typical for SiC exposed in 50% H₂O/50% O₂ at 1200°C, are shown in Figure 2a. The overall weight change is due to the sum of the weight gain due to the growth of the scale and the weight loss due to volatilization of the silica. At long times, oxide growth occurs at the same rate that oxide volatilization occurs so that a constant oxide thickness is formed while a linear weight loss is observed. Figure 2b shows the corresponding dimensional change of SiC during paralinear oxidation. The rate constants used to plot these curves are given in terms of oxide thickness rather than weight change, but are equivalent to those used in Figure 2a, so that direct comparisons may be made. Note that even after a constant oxide thickness is achieved, SiC recession continues at a linear rate as silica volatilizes. Under conditions where the volatility rate is much greater than the oxidation rate, nearly linear weight loss and recession will be observed even at short times. The rate of SiC recession is thus controlled by the volatility rate of silica rather than the oxidation rate of SiC.

The flux of volatile silicon species is limited by diffusion through a gaseous boundary layer. Boundary layer limited fluxes, J , can be calculated for a flat plate using the following equation[14]:

$$J = 0.664 \text{Re}^{1/2} \text{Sc}^{1/3} \frac{D\rho_v}{L} \quad (11)$$

where J is a mass flux, Re is the Reynolds number, Sc is the Schmidt number, D is the interdiffusion coefficient of the volatile species in the boundary layer combustion gas, ρ_v is the concentration of the volatile species at the solid/gas

interface and L is the characteristic length of the test specimen parallel to the direction of the gas flow. Expanding the Reynolds and Schmidt numbers results in:

$$J = 0.664 \left(\frac{\rho v L}{\eta} \right)^{1/2} \left(\frac{\eta}{\rho D} \right)^{1/3} \frac{D \rho_v}{L} \quad (12)$$

Here, ρ is the concentration of the boundary layer combustion gas, v is the linear gas velocity, and η is the gas viscosity. Gas concentrations are calculated from the ideal gas law. The interdiffusion coefficient is calculated using the Chapman-Enskog Equation [15] using tabulated gas constant values [16,17]. Values for silicon hydroxide and oxyhydroxide species are approximated with values for corresponding fluoride molecules or similar oxide molecules.

At higher gas velocities, laminar flow is expected to give way to turbulent conditions. In a smooth-walled tube of circular cross-section this transition occurs for Reynolds numbers, based on tube diameter Re_D , greater than 2100 [18]. A flat plate placed in turbulent flow will build up a laminar boundary layer near the leading edge. Flow along the plate will become turbulent at some distance downstream. This transition occurs at a Reynolds number, based on the distance from the leading edge Re_x , of 2×10^5 to 5×10^5 [17]. Under these conditions, the boundary layer of combustion gases is disturbed, allowing faster volatilization of the surface layers. In the limiting case, the boundary layer would be completely swept away and the volatilization rate would depend only on the vapor pressure of the volatile species, equivalent to volatilization into a vacuum.

This maximum possible mass flux can be calculated using the Langmuir Equation:

$$J = \frac{PM^{1/2}}{(2\pi RT)^{1/2}} \quad (13)$$

Here, the flux, J , is in units of mass per unit area per time, M is the molecular weight of the vapor species, R is the gas constant and T is the absolute temperature. Boundary layer calculations based on laminar flow, therefore, give minimum volatilization rates.

In the cases discussed herein, boundary layer control dominates. Equations 11 and 12 can be recast in terms of known combustion parameters, such as gas velocity, total pressure, and partial pressures of the volatile species:

$$J \propto \frac{v^{1/2}}{P_{\text{total}}^{1/2}} \sum P_{\text{volatile}} \quad (14)$$

The temperature dependence of these fluxes is contained within the partial pressure of the volatile species. The partial pressures of the volatile species can in turn be written in terms of the combustion gas phase constituents: O_2 , H_2O , H_2 , CO_2 , CO , and N_2 . Equilibrium constants can be written for reactions 4 through 9. For example,

$$K_7 = \frac{[P(\text{Si}(\text{OH})_4)]}{[P(\text{H}_2\text{O})]^2} \quad (15)$$

From this simple expression it can be seen that the $P(\text{Si}(\text{OH})_4)$ depends on the square of the water vapor pressure. It follows, then, that for volatility due to $\text{Si}(\text{OH})_4$ formation:

$$J_{\text{Si(OH)}_4} \propto \frac{V^{1/2}}{P_{\text{total}}^{1/2}} P(\text{H}_2\text{O})^2 \quad (16)$$

Mass fluxes obtained at a given temperature can thus be easily extrapolated to those at other gas pressures and velocities once the correct volatile formation reactions are identified. For each volatile species, the velocity exponent is predicted to be 1/2. However, the pressure and temperature dependence of each species will vary, and these dependencies are summarized in Table 1.

The probable identity of the volatile species present in various combustion environments is made by comparing the overall magnitude of the fluxes, the pressure dependence, and the temperature dependence of the measured data to calculated values under the same conditions. Thermodynamic data can be used to predict vapor pressures of volatile species, which can in turn be used in Equations 11 and 12 to calculate boundary layer controlled fluxes of volatile species. While thermodynamic data for SiO(g) are readily available [19], data for hydroxides and oxyhydroxides are more limited. Hashimoto [7] has experimentally determined limited thermodynamic quantities for Si(OH)₄(g) while Hildenbrand and Lau [9,10] have experimentally determined limited thermodynamic data for the SiO(OH)(g) and SiO(OH)₂(g) species. It was, therefore, necessary to make use of several sets of estimated thermodynamic quantities [11,20] to calculate fluxes of the silicon oxyhydroxide species. The thermochemical data of Krikorian [11] are based on equilibrium constants for volatilization reactions from a compilation of studies as well as entropies calculated from spectral data and partition functions. The thermochemical data

of Allendorf et al. [20] and Darling and Schlegel [21] are derived from ab initio calculations using Hartree-Fock theory.

The aim of this paper is to use the available thermodynamic data and flux calculations to develop a self-consistent model for the volatilization of silica during paralinier oxidation of SiC in combustion environments. The experimental process [1,13,22] should be described with as accurate a chemical model as possible. Verification of this model will thereby enable the prediction of SiC recession under a variety of combustion conditions.

PROCEDURE

Experimental data from three sources were examined in light of possible SiO₂ volatilization/SiC recession reactions. These studies are the HPBR fuel-rich and fuel-lean conditions from Part I of this paper, synthetic fuel-lean furnace tests [13], and synthetic fuel-rich furnace tests [22]. Synthetic gas mixtures are premixed to reflect the components found in combustion gas environments. For example, the synthetic fuel lean mixture models the oxygen and water vapor found at $\phi=0.6$ and a total pressure of 5 atm, while the synthetic fuel-rich mixture models the combustion gas products at $\phi=1.5$. The experimental parameters used in the calculations are shown in Table 2.

The available thermodynamic data for volatile Si-O-H species have been adapted for use in ChemSage [23], a free energy minimization program. The free energy expressions for the species added to the ChemSage data base are shown in the Appendix. Data for SiO are from JANAF [19], data for Si(OH)₄

have been experimentally determined by Hashimoto [7], and two sets of estimated data for $\text{SiO}(\text{OH})$ and $\text{SiO}(\text{OH})_2$ [11,20] were also used. Additional data for $\text{SiO}(\text{OH})$ by Darling and Schlegel [21] are referred to, but not used in the calculations. SiO_2 (cristobalite) plus the combustion gas composition at the experimental temperature and pressure were input to ChemSage [23]. The calculations were each repeated with the two data sets specified in Table 3. Vapor pressures of SiO , $\text{Si}(\text{OH})_4$, $\text{SiO}(\text{OH})$, and $\text{SiO}(\text{OH})_2$ were calculated in each case. The vapor pressure of $\text{Si}_2\text{O}(\text{OH})_6$ was found to be negligible under the conditions of this study.

Boundary layer controlled fluxes of the volatile species were then calculated using the ChemSage vapor pressures in Equation 12. The boundary layer thicknesses, δ , for the low gas velocity experiments were calculated to vary between 0.69 and 0.75 cm for the synthetic fuel-lean furnace experiments [13] and between 2.2 and 2.6 cm for the synthetic fuel-rich furnace experiments [22] using the expression [24]:

$$\delta = \frac{1.5L}{\text{Re}^{1/2} \text{Sc}^{1/3}} \quad (17)$$

All terms are the same as in Equation 11. Since the furnace tube inner radius is 1.1 cm, boundary layers of the sizes calculated above using Equation 17 are physically impossible. For these cases, fluxes of volatile species were calculated by restricting the boundary layer to half the furnace tube radius, 0.5 cm, using the following expression [24]:

$$J = \frac{Dp_v}{\delta} \quad (18)$$

Again all terms are defined as in Equation 12. Restricted boundary layers result in measured fluxes higher than those calculated using Equation 12.

The calculated fluxes were compared to experimentally measured fluxes. Chemical models for volatilization were chosen which best represented the experimental data. These models were then used to extrapolate from furnace test conditions to HPBR conditions using expressions such as Equation 16.

RESULTS

The calculated boundary layer controlled fluxes are listed in Table 4. Contributions of each species to the total flux are specified. Calculated fluxes are compared to experimental results under each test condition. The magnitude of the fluxes as well as the pressure and temperature dependence are used to evaluate whether the boundary layer calculations adequately describe the measured fluxes and which Si-O-H species are likely contributing to the SiO₂ volatility/SiC recession. Calculated Langmuir fluxes are several orders of magnitude larger than measured fluxes in all cases, demonstrating that a gaseous boundary layer acts as a barrier to volatilization.

Synthetic Fuel-Lean Conditions

Experimental results [13] as well as calculated fluxes for synthetic fuel-lean furnace conditions are shown in Figure 3. Calculated boundary layer controlled fluxes of Si(OH)₄ based on Hashimoto's [7] measured thermodynamic data agree with experimentally measured fluxes. Data set K indicates that SiO(OH)₂ should also be forming in measurable quantities, whereas data set A

predicts negligible vapor pressures of this volatile species. Use of data set K in the flux calculations results in a larger overall flux of volatile species as well as a larger temperature dependence than that found experimentally. Thus, the synthetic fuel-lean furnace experimental results agree best with boundary layer controlled fluxes of an $\text{Si}(\text{OH})_4$ volatile species alone.

Fuel-Lean Burner Rig

Experimental results [1] and calculated boundary layer controlled fluxes for HPBR fuel-lean conditions are shown in Figure 4. Data set K predicts that $\text{SiO}(\text{OH})_2$ will be important in addition to $\text{Si}(\text{OH})_4$ while data set A predicts that only $\text{Si}(\text{OH})_4$ is important under these conditions. The experimental data fall between the predictions in both magnitude and activation enthalpy. This suggests that $\text{SiO}(\text{OH})_2$ is present, but in quantities intermediate to those predicted by Krikorian and Allendorf.

The pressure exponent for the volatilization rate in the HPBR fuel-lean case was found to be 1.50 ± 0.13 . While this is in exact agreement with the predicted pressure dependence in the case of $\text{Si}(\text{OH})_4$ formation (Equation 16), this result is not consistent with the presence of appreciable amounts of $\text{SiO}(\text{OH})_2$. Therefore, the pressure dependence indicates that $\text{Si}(\text{OH})_4$ is the predominant volatile species in fuel-lean combustion conditions.

Synthetic Fuel-Rich Conditions

Experimental results [22] and calculated fluxes for synthetic fuel-rich furnace conditions are shown in Figure 5. Calculated boundary layer controlled fluxes of SiO agree best with both the magnitude and temperature dependence

of the experimental data. While Si(OH)_4 is predicted to be more important than SiO , and the magnitude of the calculated volatility rate based on both species fits the data quite well, the temperature dependence of the sum of these fluxes (220 kJ/mol) is not large enough to adequately describe the data (473 ± 195 kJ/mol). Data set K predicts that the formation of SiO is negligible but that SiO(OH) and SiO(OH)_2 dominate the volatility of SiO_2 under these conditions. In contrast, data set A predicts that Si(OH)_4 is the primary volatile species at 1500K, SiO is the primary species at 1700K, while SiO(OH)_2 is only found in small amounts at 1700K. In summary, the synthetic fuel-rich furnace experimental results agree best with boundary layer controlled fluxes of an SiO volatile species alone, although silicon hydroxide and oxyhydroxide species may form in measurable amounts.

Fuel-Rich Burner Rig

Finally, experimental results [1] and calculated boundary layer controlled fluxes for HPBR fuel-rich conditions are shown in Figure 6. Data set K predicts that Si(OH)_4 , SiO(OH)_2 , and SiO(OH) are all important. Si(OH)_4 is most important at 1500K while SiO(OH) is most important at 1700K. On the other hand, data set A predicts that only Si(OH)_4 and SiO are important under these conditions. SiO is predicted to become significant only at 1700K. The experimental data agree quite well in *magnitude* with the predictions of data set K although the temperature dependence of the measured values is significantly less than the predicted values. The magnitude of the measured flux is significantly higher than that predicted using data set A which predicts the

oxyhydroxides are unimportant. This suggests that one or both oxyhydroxide species are important under these conditions.

The pressure exponent for the volatilization rate in the HPBR fuel-rich case was found to be 1.74 ± 0.20 . Because multiple volatile species are expected to be present in this environment, it was attempted to isolate the pressure effects of $\text{Si}(\text{OH})_4$ from the remaining species. This is shown in Figure 7a. The flux due to $\text{Si}(\text{OH})_4$ at 1651K and several pressures was calculated using Hashimoto's data [7]. This calculated value was subtracted from the measured value. The remaining pressure dependence of 2.03 was attributed to other volatile species. Several observations can be made from this plot. First, $\text{Si}(\text{OH})_4$ makes up only a small fraction of the volatile products formed under these conditions. And second, the pressure exponent of 2.03 necessarily implies that the unknown volatile species have a stronger dependence on water vapor pressure than $\text{Si}(\text{OH})_4$. This contradicts the previous conclusion that the unknown volatile species are $\text{SiO}(\text{OH})$ and/or $\text{SiO}(\text{OH})_2$ which have flux related pressure exponents of $-1/4$ and $1/2$ respectively. The expected pressure exponent for $\text{Si}_2(\text{OH})_6$ flux from Equation 10 is 2.0. Note also that this molecule would likely be formed in fuel-rich environments and not in fuel-lean environments due to the oxygen generated as a product of Reaction 10. While Krikorian [11] has calculated free energy functions for this molecule, no enthalpy data are available. Estimation of the vapor pressure of this species may be possible, but is beyond the scope of this paper.

The reaction enthalpy for SiO_2 volatility in the HPBR fuel-rich case was found to be 159 ± 9 kJ/mol. Again, because multiple volatile species are expected to be present in this environment, it was attempted to isolate the temperature effects of Si(OH)_4 and SiO from the remaining species. This is shown in Figure 7b. The flux due to Si(OH)_4 and SiO at 1500, 1600, and 1700K was calculated. This calculated value was subtracted from the measured value. The remaining flux had a reaction enthalpy of 170 kJ/mol which can be attributed to the formation of other volatile species from SiO_2 . It can be seen from Table 1b that the enthalpies of reaction for both SiO(OH)_2 and SiO(OH) formation are much higher than 170 kJ/mol. This again indicates that some other volatile species is needed to explain the high pressure fuel-rich results. While the reaction enthalpy of $\text{Si}_2(\text{OH})_6$ by reaction 10 is unknown, entropy considerations (Reaction 10 results in a net loss of vapor molecules) necessitate that the reaction enthalpy be relatively low compared to reactions 6 and 9 [25]. This is in qualitative agreement with the fuel-rich HPBR results.

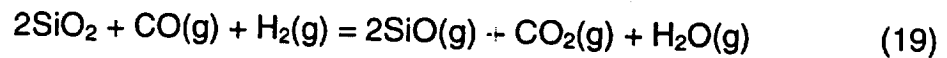
Extrapolation of Laboratory Furnace Results to HPBR Conditions

The simple volatilization models developed for the synthetic combustion gas furnace tests and the experimental variables of pressure and velocity are now used to extrapolate to the volatilization rates under HPBR conditions. Comparisons to measured HPBR volatilization rates are made. These results are shown in Figures 8a and 8b.

For the fuel-lean case assuming Si(OH)_4 formation only, Equation 16 was used to extrapolate volatilization rates from 50% H_2O at 1 atm total pressure and

a gas velocity of 4.4 cm/sec to 12.3% H₂O (for $\phi=0.9$) at 6.3 atm total pressure and a gas velocity of 20 m/sec. This extrapolation is labeled (1) in Figure 8a. The extrapolation somewhat over-predicts the magnitude of the volatility and under-predicts the temperature dependence. Nevertheless, the extrapolation gives a fair prediction of the order of magnitude of the volatility rates measured in the HPBR in fuel-lean conditions.

Previous discussion has shown that the synthetic fuel-rich furnace tests are best modeled by SiO volatility, but this model is inadequate to explain the HPBR results. The following discussion shows the shortfall in predicted volatility when using the one atmosphere model to predict volatility at the conditions of the HPBR. In the fuel-rich environment, the reducing species present in the combustion environment, CO and H₂, play a significant role in the silica volatility. The dependence of SiO on the partial pressures of combustion gases similar to Equation 16 must be formulated. The reactions for SiO formation given by Equations 4 and 5 have therefore been summed for this simple model of the combustion environment:



The flux of SiO(g) for this model can then be expressed as:

$$J_{\text{SiO}} \propto \frac{v^{1/2}}{P_{\text{total}}^{1/2}} \sqrt{\frac{(P_{\text{CO}})(P_{\text{H}_2})}{(P_{\text{CO}_2})(P_{\text{H}_2\text{O}})}} \quad (20)$$

and since the partial pressures of the gaseous components at a constant ϕ scale with each other as total pressure changes:

$$J_{\text{SiO}} \propto \frac{v^{1/2}}{P_{\text{total}}^{1/2}} \text{ at constant } \phi \quad (21)$$

At constant ϕ and gas velocity, the SiO(g) flux should thus decrease as the total pressure is increased. This behavior differs from that of Si(OH)₄ and SiO(OH)₂.

Equation 20 was used to extrapolate volatilization rates based on SiO volatility from a synthetic ϕ of 1.5 at 1 atm total pressure and a gas velocity of 0.4 cm/sec to $\phi=1.8$ at 6.3 atm total pressure and a gas velocity of 20m/sec. This extrapolation is labeled (2) in Figure 8b. While the formation of SiO(g) explains the results for the furnace testing in synthetic fuel-rich conditions, it is clearly inadequate to explain the volatility observed in fuel-rich conditions at the higher pressures in the HPBR.

Since the thermochemical data predict that Si(OH)₄ is also present in fuel-rich environments, the synthetic fuel-lean volatility measured at 1 atm was used to extrapolate Si(OH)₄ formation to the HPBR fuel-rich conditions. Equation 16 was used to extrapolate volatilization rates from 50% H₂O at 1 atm total pressure and a gas velocity of 4.4 cm/sec to 10.3% H₂O (for $\phi=1.8$) at 6.3 atm total pressure and a gas velocity of 20 m/sec. This extrapolation is labeled (3) in Figure 8b. The extrapolated values for SiO and Si(OH)₄, curves (2) and (3), are then summed and shown as curve (4) in Figure 8b. This extrapolation of SiO and Si(OH)₄ from furnace testing to the HPBR fuel-rich conditions under-predicts the magnitude of the volatility of silica under these conditions. This extrapolation again shows that other volatile silicon-containing species, such as SiO(OH)₂,

SiO(OH) , and/or $\text{Si}_2(\text{OH})_6$ may be important in fuel-rich combustion environments at high pressures.

DISCUSSION

A gaseous diffusion model has been used to describe the volatility of SiO_2 scales formed on SiC under combustion conditions. The temperature, pressure, and velocity dependencies as well as the overall magnitude of the volatilization rate conform to this basic model. However, exact agreement between the calculated and measured fluxes is not always obtained. Concerns with the deficiencies of the input thermodynamic data and the gaseous diffusion model itself are now discussed.

Assessment of Thermodynamic Data

The accuracy of prediction based on the formation of a particular volatile species depends on the accuracy of the thermochemical data. Much of the thermochemical data for the Si-O-H system has not been measured experimentally or is incomplete. In this section, we attempt to evaluate the accuracy of the *experimental* data with reference to our own laboratory observations. Then, in turn, we attempt to evaluate the *estimated* and *calculated* data with reference to any available *experimental* data. Clearly, additional experimental measurements of thermochemical data for the silicon oxyhydroxide species would be helpful to characterize the volatilization/recession processes of SiO_2/SiC system in combustion environments.

Si(OH)₄: Comparison of furnace tests to Hashimoto's [7] experimentally-determined thermochemical data

The vapor pressures of Si(OH)₄ predicted from Hashimoto's transpiration studies are consistently higher than those observed in our laboratory (by less than an order of magnitude). Our results are probably lower due to partial suppression of SiO₂ volatility from the fused quartz reaction tubes used in our studies. This mechanism of partially suppressed volatility should not affect the HPBR results in our test, where no other Si-base materials were present.

Si(OH)₄: Comparison of estimated and calculated thermochemical data to measured thermochemical data.

The free energy of formation for Si(OH)₄ at 1600K from Hashimoto's [7] experimental study as well as Krikorian's [11] and Allendorf's [20] calculated values are shown in Table 5. All three values are in fairly good agreement with each other. Krikorian's values slightly under-predict the stability of Si(OH)₄ whereas Allendorf's values slightly over-predict Si(OH)₄ stability. Hashimoto's experimentally determined values were used in all models in this study.

SiO(OH)₂ and SiO(OH): Comparison of estimated and calculated thermochemical data to experimental observations.

Qualitative observations in our laboratory [8] using a specialized molecular beam mass spectrometer for the reaction of silica and water vapor at 1300°C and 1 atmosphere total pressure support the conclusion that both Si(OH)₄ and SiO(OH)₂ should be observed in appreciable quantities when SiC is present in combustion environments. The intensity of SiO(OH)₂ was observed in quantities

ten times less than $\text{Si}(\text{OH})_4$ under conditions where Krikorian's data [11] predict a vapor pressures of $\text{SiO}(\text{OH})_2$ three times that of $\text{Si}(\text{OH})_4$ and Allendorf's data [20] predicts $\text{SiO}(\text{OH})_2$ vapor pressures about thirty times less than those of $\text{Si}(\text{OH})_4$. Hashimoto [7] observed a square dependence of volatile species on the water vapor partial pressure for temperatures between 1100 and 1500°C under similar conditions to those studied using mass spectrometry, indicating that $\text{Si}(\text{OH})_4$ is the primary volatile species. The combination of these results indicates that $\text{SiO}(\text{OH})_2$ is present in silica-containing combustion environments in measurable quantities but in amounts about midway between the predictions of Krikorian's and Allendorf's data. At temperatures higher than 1300°C, $\text{SiO}(\text{OH})_2$ will become more significant relative to $\text{Si}(\text{OH})_4$ due to the difference in the temperature dependence of the formation reactions. At higher pressures $\text{SiO}(\text{OH})_2$ will become less important relative to $\text{Si}(\text{OH})_4$ due to its smaller pressure dependence.

SiO(OH)₂ and SiO(OH): Comparison of estimated and calculated thermochemical data to measured thermochemical data.

The free energy of formation of $\text{SiO}(\text{OH})_2$ and $\text{SiO}(\text{OH})$ from Krikorian's [11] and Allendorf's [20] calculated values as well as the experimentally determined values of Hildenbrand and Lau [9,10] at 2065K are shown in Table 6. This temperature is the only temperature at which experimentally determined data are available. Hildenbrand and Lau's values were obtained using Knudsen effusion mass spectrometry. Krikorian's estimates are quite close to the measured values for both molecules, but slightly over-predict the stability of the

oxyhydroxides. Allendorf's calculated free energies significantly under-predict the stability of both oxyhydroxide molecules. There is some lingering uncertainty regarding the experimentally determined values for SiO(OH) due to the complex fragmentation patterns occurring during mass spectrometry [20,10]. Allendorf [20] and Darling&Schlegel [21] calculated stability of SiO(OH) are in better agreement with Hildenbrand and Lau's revised values for SiO(OH) [10] than Krikorian's estimate. This revision results in a higher temperature dependence for reaction 9.

Flow Conditions in the HPBR

While the gas flow conditions in the furnace tests are well defined and fall well within the laminar flow regime, the gas flow conditions in the HPBR are more complicated and require some discussion. First, Reynold's numbers (Re_D) calculated for nitrogen flow in the burner rig are about 8×10^4 , indicating turbulent flow conditions [18]. Re_x calculated for a flat plate geometry, similar to a SiC coupon in the burner rig, is on the order of 1×10^4 . For Re_x less than 10^5 , flat plate samples within the turbulent flow of the burner rig should develop a laminar flow boundary layer given a well defined velocity profile [18]. However, since the burner rig essentially has the geometry of a short pipe (length to diameter ratio is less than 10), entry effects are important and a well defined velocity profile is not yet established as the flow impinges on the SiC sample under test [14]. Use of either laminar or turbulent flow equations under these conditions may not apply. Finally, when turbulent flow is established, the Re exponent in the flux equation is 0.8 [17]. Thus, the velocity exponent is expected

to vary between 0.5 for laminar flow and 0.8 for turbulent flow. The regression of the SiC recession rates in the HPBR yielded velocity exponents of 0.50 ± 0.16 for the fuel-lean case and 0.69 ± 0.32 in the fuel rich case. The fuel-lean velocity exponent is in excellent agreement with the predicted laminar flow velocity exponent of 0.5. The fuel-rich velocity exponent, while not statistically significantly different from 0.5, may indicate that laminar flow equations do not apply under these conditions. This may explain the difficulty encountered in modeling the fuel-rich volatility chemistry using laminar flow equations.

Volatile Species Found for SiC in Fuel-Lean Combustion Conditions

The volatilization and recession process for the SiO_2/SiC system in fuel-lean combustion conditions has been well characterized in this study. A summary of the identification of the volatile species based on magnitude of flux as well as pressure and temperature dependence is found in Table 7. Laminar flow analyses appear to adequately model the process. Volatilization of silica can be adequately explained by the formation of $\text{Si}(\text{OH})_4$ alone. There is some evidence that $\text{SiO}(\text{OH})_2$ is also formed under these conditions in measurable quantities. The importance of $\text{SiO}(\text{OH})_2$ will increase with temperature and decrease with pressure.

Volatile Species Found for SiC in Fuel-Rich Combustion Conditions

The volatilization and recession process for the SiO_2/SiC system in fuel-rich combustion conditions is still not completely understood. The likely identity of the volatile species formed under these conditions based on the magnitude of the flux, the temperature dependence and the pressure dependence is also

summarized in Table 7. Volatilization at low pressures in the fuel-rich combustion environment (1 atm) can be attributed to the formation of SiO. Since the flux of this species decreases as total pressure is increased, it is not surprising that completely different volatile species are needed to explain the results at higher pressures. It is therefore difficult to model high pressure fuel-rich combustion environments in a one atmosphere furnace test. In addition, laminar flow may not be operative under the high pressure conditions studied here. The high pressure fuel-rich volatility mechanism is best described, given the current thermochemical data, by the formation of Si(OH)_4 , SiO(OH) , and SiO(OH)_2 . SiO(OH) is expected to increase with importance as the temperature is raised and as the combustion environment becomes more fuel-rich. The $\text{Si}_2(\text{OH})_6$ species satisfies the pressure dependence of the SiO_2 volatilization rate observed here, but little is known about this molecule. Despite the uncertainty in the chemical model for silica volatility in fuel-rich conditions, the multiple linear regression model (volatility rate expressed as a function of pressure, temperature, and velocity) obtained in Part I of this paper is useful to estimate the volatility rate in fuel-rich combustion environments.

Conclusions

Water vapor is responsible for the degradation of SiC in the fuel-lean environment. Silica volatility in fuel-lean combustion environments is attributed primarily to the formation of $\text{Si(OH)}_4(\text{g})$ with a small contribution of $\text{SiO(OH)}_2(\text{g})$. Water vapor in combination with the more reducing environment contributes to

the higher rates of degradation of SiO_2 in fuel-rich combustion conditions. Silica volatility in a fuel-rich combustion environment is best described by the formation of $\text{SiO}(\text{g})$ at one atmosphere total pressure and greater contributions from the formation of $\text{Si}(\text{OH})_4(\text{g})$, $\text{SiO}(\text{OH})_2(\text{g})$, and $\text{SiO}(\text{OH})(\text{g})$ at higher pressures. The molecule, $\text{Si}_2(\text{OH})_6(\text{g})$, would provide the correct pressure dependence of the volatility of SiO_2 under fuel-rich conditions, however, complete thermochemical data are unavailable for this species. Clearly the need exists for more experimental measurements of thermochemical data for the Si-O-H system to aid in the modeling of silica volatility in combustion environments.

Acknowledgments

The authors would like to thank Suleyman Gogoklu of NASA Lewis Research Center for many helpful discussions on gas phase transport.

References

1. R.C. Robinson and J.S. Smialek, SiC Recession due to SiO_2 Scale Volatility under Combustor Conditions. Part I: Experimental Results and Empirical Model, this journal.
2. N.S. Jacobson, Corrosion of Silicon-Based Ceramics in Combustion Environments, J. Am. Ceram. Soc., 76 [1] 3-28 (1993).
3. E.J. Opila and Q.N. Nguyen, The Oxidation of CVD Silicon Carbide in Carbon Dioxide, accepted for publication in J. Am. Ceram. Soc.

4. E.J. Opila and Jacobson, SiO(g) Formation from SiC in Mixed Oxidizing-Reducing Gases, *Oxid. Metals* 44 [5/6] 527-544 (1995).
5. H.-E. Kim and D.W. Ready, pp. 301-312 in *Silicon Carbide '87*, J.D. Cawley and C.E. Semler, eds., American Ceramic Society, Westerville, OH, 1987.
6. T. Narushima, T. Goto, Y. Yokoyama, Y. Iguchi, and T. Hirai, High-Temperature Active Oxidation of Chemically Vapor-Deposited Silicon Carbide in CO-CO₂ Atmosphere, *J. Am. Ceram. Soc.* 76 [10] 2521-2524 (1993).
7. A. Hashimoto, "The Effect of H₂O Gas on Volatilities of Planet-Forming Major Elements: I. Experimental Determination of Thermodynamic Properties of Ca-, Al-, and Si-Hydroxide Gas Molecules and its Application to the Solar Nebula," *Geochim. Cosmochim. Acta* 56, 511-32 (1992).
8. E.J. Opila, D.S. Fox, and N.S. Jacobson, Mass Spectrometric Identification of Si-O-H(g) Species from the Reaction of Silica with Water Vapor, *J. Am. Ceram. Soc.* 80 [4] 1009-1012 (1997).
9. D.L. Hildenbrand and K.H. Lau, "Thermochemistry of Gaseous SiO(OH), SiO(OH)₂, and SiO₂," *J. Chem. Phys.* 101 [7] 6076-9 (1994).
10. D.L. Hildenbrand and K.H. Lau, "Revision of Thermochemical Data for SiO(OH)(g)," submitted to *J. Chem. Phys.*
11. O.H. Krikorian, "Thermodynamics of the Silica-Steam System," in *Symposium on Engineering with Nuclear Explosives*, January 14-16, 1970, Las Vegas, NV, vol. 1, p. 481, (1970), unpublished.
12. C.S. Tedmon, Jr., "The Effect of Oxide Volatilization on the Oxidation Kinetics of Cr and Fe-Cr Alloys," *J. Electrochem. Soc.*, 113 [8] 766-68 (1967).

13. E.J. Opila and R.E. Hann, "Paralinear Oxidation of CVD SiC in Water Vapor," J. Am. Ceram. Soc., 80 [1] 197-205 (1997).
14. W.M. Kays and M.E. Crawford, pp. 139, 197 in Convective Heat and Mass Transfer, McGraw-Hill, Inc. Ny, NY, 1980.
15. G.H. Geiger and D.R. Poirier; p. 464 in Transport Phenomena in Metallurgy, Addison-Wesley Publishing Company, Reading, MA, 1973.
16. R.A. Svehla "Estimated Viscosities and Thermal Conductivities of Gases at High Temperatures," NASA Technical Report R-132.
17. T.K. Sherwood, R.L. Pigford, C.R. Wilke, pp. 20, 201 in Mass Transfer, McGraw-Hill, Inc., NY, NY, 1975.
18. D.R. Gaskell, pp. 31, 154 in An Introduction to Transport Phenomena in Materials Engineering, Macmillan Publishing Co., NY, 1992.
19. M.W. Chase, Jr., C.A. Davies, J.R. Downey, Jr., D.J. Frurip, R.A. McDonald, and A.N. Syverud, Editors, JANAF Thermochemical Tables, 3rd ed., American Chemical Society and American Physical Society, New York (1985).
20. M.D. Allendorf, C.F. Melius, P. Ho, and M.R. Zachariah, Theroretical Study of the Thermochemistry of Molecules in the Si-O-H System, J. Phys. Chem. 99, 15285-15293 (1995).
21. C.L. Darling and H.B. Schlegel, Heats of Formation of SiH_nO and SiH_nO_2 Calculated by ab Initio Molecular Orbital Methods t the G-2 Level of Theory, J. Phys. Chem. 97, 8207-8211 (1993).
22. D.S. Fox, E.J. Opila, and R.E. Hann, Paralinear Oxidation of CVD SiC in Simulated Fuel-Rich Combustion, submitted to J. Am. Ceram. Soc.

23. G. Eriksson and K. Hack, ChemSage - A Computer Program for the Calculation of Complex Chemical Equilibria, *Met. Trans. B*, 21B, 1013 (1990).
24. H.C. Graham and H.H. Davis, Oxidation/Vaporization Kinetics of Cr_2O_3 , *J. Am. Cer. Soc.*, 54, 89 (1971).
25. A.W. Searcy, "Entropy and High-Temperature Physical and Chemical Processes," pp. 15-32 in Chemical and Mechanical Behavior of Inorganic Materials, Wiley-Interscience, NY, 1970.

Table 1a
Pressure Dependence of Si-O-H(g) Species

Reaction number	Species	$P(\text{Si-O-H})_{\infty}(P_{\text{total}})^n$	$J(\text{Si-O-H})_{\infty}(P_{\text{total}})^m$
6	$\text{SiO}(\text{OH})_2$	$n=1$	$m=0.5$
7	$\text{Si}(\text{OH})_4$	$n=2$	$m=1.5$
8	$\text{Si}_2\text{O}(\text{OH})_6$	$n=3$	$m=2.5$
9	$\text{SiO}(\text{OH})$	$n=0.25$	$m=-0.25$
10	$\text{Si}_2(\text{OH})_6$	$n=2.5$	$m=2$

Table 1b
Temperature Dependence of Si-O-H(g) Species,
Reaction Enthalpy for $\text{SiO}_2 + \text{H}_2\text{O} = \text{Si-O-H(g)}$

Species	Source for Thermochemical Data	Reaction Enthalpy, kJ/mol
$\text{Si}(\text{OH})_4$	Hashimoto*	57
	Krikorian	32
	Allendorf	60
$\text{SiO}(\text{OH})_2$	Hildenbrand*	260
	Krikorian	247
	Allendorf	346
$\text{SiO}(\text{OH})$	Hildenbrand*	530
	Hildenbrand revised*	670
	Krikorian	524
	Allendorf	713
	Darling & Schlegel	721

*experimentally determined, all others estimated or calculated

Table 2
Parameters used for calculation of boundary layer controlled fluxes.

	Total Pressure (atm)	Linear Gas Velocity (m/sec)	Gas Composition
synthetic fuel-lean $\phi=0.6$, $P_{\text{total}}=5$ atm	1	4.4×10^{-2}	0.5 O ₂ 0.5 H ₂ O
synthetic fuel-rich $\phi=1.5$	1	4.4×10^{-3}	0.072 CO ₂ 0.100 H ₂ O 0.099 CO 0.045 H ₂ 0.684 N ₂
HPBR fuel-lean $\phi=0.9$	6.3	20	0.110 CO ₂ 0.021 O ₂ 0.123 H ₂ O 0.746 N ₂
HPBR fuel-rich $\phi=1.8$	6.3	20	0.036 CO ₂ 0.098 H ₂ O 0.162 CO 0.103 H ₂ 0.601 N ₂

Table 3
Thermochemical Data Sets Used for Flux Calculations

	Source of Thermochemical Data	
Species	Data Set K	Data Set A
Si(OH) ₄	Hashimoto	Hashimoto
SiO	JANAF	JANAF
SiO(OH) ₂	Krikorian	Allendorf
SiO(OH)	Krikorian	Allendorf

Table 4
Calculated Boundary Layer Controlled Fluxes
(mg/cm² h)

	Synthetic Fuel-Lean		Synthetic Fuel-Rich		HPBR Fuel-Lean		HPBR Fuel-Rich	
	Set K	Set A	Set K	Set A	Set K	Set A	Set K	Set A
1500K	SiO(OH)	2.69e-6	--	5.33e-4	--	1.28e-5	5.25e-3	--
	SiO(OH) ₂	3.54e-3	1.98e-6	7.07e-4	3.93e-7	1.61e-2	1.07e-2	6.22e-6
	SiO	--	--	4.62e-6	4.62e-6	--	2.88e-5	2.88e-5
1600K	Si(OH) ₄	2.85e-3	2.85e-3	1.06e-4	1.06e-4	1.98e-2	9.58e-3	9.58e-3
	SiO(OH)	3.84e-5	--	3.82e-3	--	1.74e-4	3.71e-2	--
	SiO(OH) ₂	1.26e-2	1.14e-5	2.55e-3	2.30e-6	5.46e-2	3.82e-2	3.40e-5
	SiO	--	--	6.36e-5	6.36e-5	--	3.84e-4	3.84e-4
1700K	Si(OH) ₄	3.98e-3	3.98e-3	1.57e-4	1.57e-4	2.61e-2	1.42e-2	1.42e-2
	SiO(OH)	4.03e-4	--	2.24e-2	--	1.73e-3	2.07e-1	--
	SiO(OH) ₂	3.88e-2	5.11e-5	8.15e-3	1.07e-5	1.58e-1	1.16e-1	1.58e-4
	SiO	--	--	6.62e-4	6.62e-4	--	3.95e-3	3.95e-3
	Si(OH) ₄	5.28e-3	5.28e-3	2.25e-4	2.25e-4	3.34e-2	1.83e-2	1.83e-2

A fixed boundary layer of 0.5 cm was assumed for all furnace test flux calculations.

Table 5
The free energy of formation for Si(OH)_4

ΔG°_f (1600K) kJ/mol		
Hashimoto	Krikorian	Allendorf
-782.19	-761.34	-797.47

Table 6
The free energy of formation for SiO(OH) and SiO(OH)_2

ΔG°_f (2065K) kJ/mol			
	Hildenbrand & Lau	Krikorian	Allendorf
SiO(OH)	-436.45 (-299.05)*	-450.78	-254.39
SiO(OH)_2	-525.66	-546.65	-454.38

*revised value

Table 7
Probable Identification of Volatile Species in Combustion Environments

	Criteria for choice of volatile species	Most likely volatile species
Synthetic fuel-lean	magnitude of flux T dependence of flux	Si(OH)_4 Si(OH)_4
Synthetic fuel-rich	magnitude of flux T dependence of flux	SiO SiO
HPBR fuel-lean	magnitude of flux T dependence of flux P dependence of flux	Si(OH)_4 , SiO(OH)_2 Si(OH)_4 , SiO(OH)_2 Si(OH)_4
HPBR fuel-rich	magnitude of flux T dependence of flux P dependence of flux	SiO(OH) , SiO(OH)_2 , Si(OH)_4 $\text{Si}_2(\text{OH})_6(?)$, Si(OH)_4 $\text{Si}_2(\text{OH})_6$, Si(OH)_4

Appendix
Thermochemical Expressions for Volatile Species Used in ChemSage

The following is a compilation of the free energy expressions used in ChemSage for calculation of partial pressures of volatile Si-O-H(g) species under combustion conditions. Note that in ChemSage, contrary to SolGasMix, the Standard Element Reference (SER) state is defined as the stable phase at 298K rather than the stable phase at the temperature of interest. The Gibbs energy equation is of the following form: $G(T) = A + B \cdot T + C \cdot T \cdot \ln T + D \cdot T^2 + E \cdot T^3 + F/T$.

Species	Source	A	B	C	D	E	F
Si(OH) ₄	Hashimoto	-1.37229E+06	5.06064E+02	-1.25752E+02	-1.59765E-02	6.52809E-07	-1.33145E+06
SiO	JANAF	-1.153070E+05	3.988578E+01	-3.664745E+01	-3.016475E-04	9.317488E-09	7.200307E+05
SiO(OH) ₂	Krikorian	-9.32119E+05	3.32737E+02	-9.10899E+01	-9.53907E-03	3.31410E-07	-3.14321E+05
SiO(OH)	Krikorian	-5.23173E+05	1.79359E+02	-6.53519E+01	-6.02243E-03	1.67320E-07	6.27915E+04
SiO(OH) ₂	Allendorf	-8.39113E+05	3.32935E+02	-9.10899E+01	-9.53907E-03	3.31410E-07	-3.14321E+05
SiO(OH)	Allendorf	-3.44378E+05	1.88591E+02	-6.53519E+01	-6.02243E-03	1.67320E-07	6.27915E+04

List of Figures

Figure 1. Equilibrium calculation of gas products from combustion of Jet A fuel and air as a function of equivalence ratio, ϕ .

Figure 2. Paralinear oxidation kinetics for SiC in water vapor. Rate constants are typical of those found for 50% H₂O/50% O₂ at 1 atm total pressure, gas velocity of 4.4 cm/s, and temperature of 1200°C. A) Weight change kinetics. B) Dimensional change kinetics.

Figure 3. Linear weight loss rates for SiC in synthetic fuel-lean conditions. The dashed line shows the measured rates while the solid lines show calculated rates.

Figure 4. Linear weight loss rates for SiC in fuel-lean conditions in the HPBR. The dashed line shows the measured rates while the solid lines show calculated rates.

Figure 5. Linear weight loss rates for SiC in synthetic fuel-rich conditions. The dashed line shows the measured rates while the solid lines show calculated rates.

Figure 6. Linear weight loss rates for SiC in fuel-rich conditions in the HPBR. The dashed line shows the measured rates while the solid lines show calculated rates.

Figure 7. A) Pressure dependence (at about 1650K) and B) Temperature dependence of the flux of the unknown Si-O-H species from SiC in high-pressure fuel-rich conditions.

Figure 8. Comparison of weight loss rates for SiC measured in the HPBR to those extrapolated from furnace results based on A) Si(OH)_4 in fuel-lean conditions, and B) $\text{SiO} + \text{Si(OH)}_4$ in fuel-rich conditions.

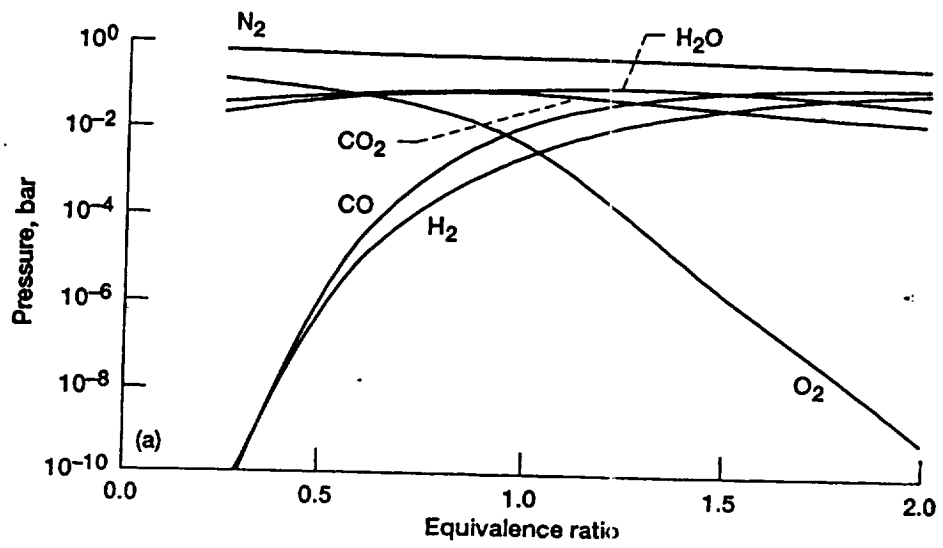
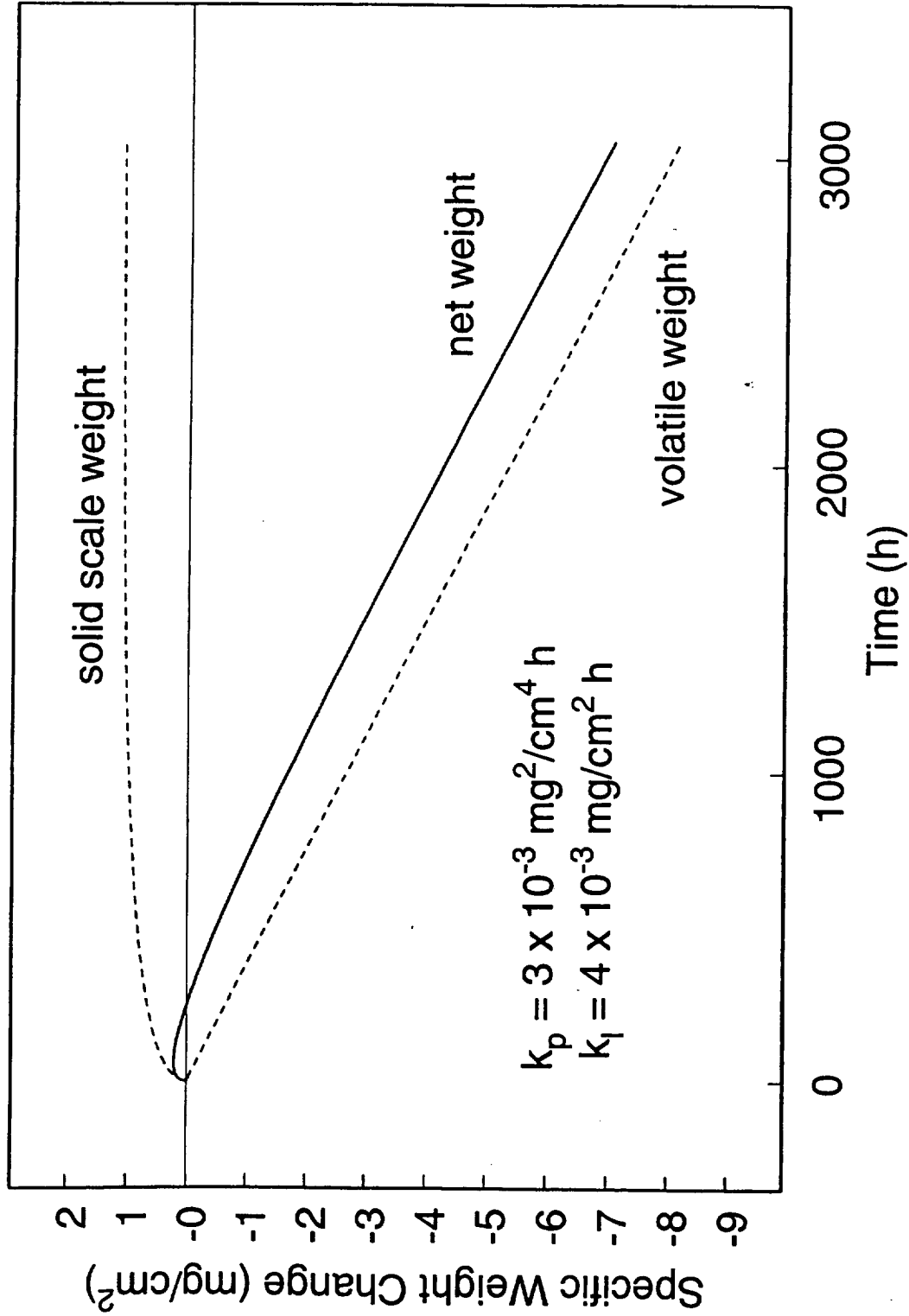


Fig. 1

Paralinear Weight Change for SiC in Water Vapor



Paralinear Oxide Growth for SiC in Water Vapor

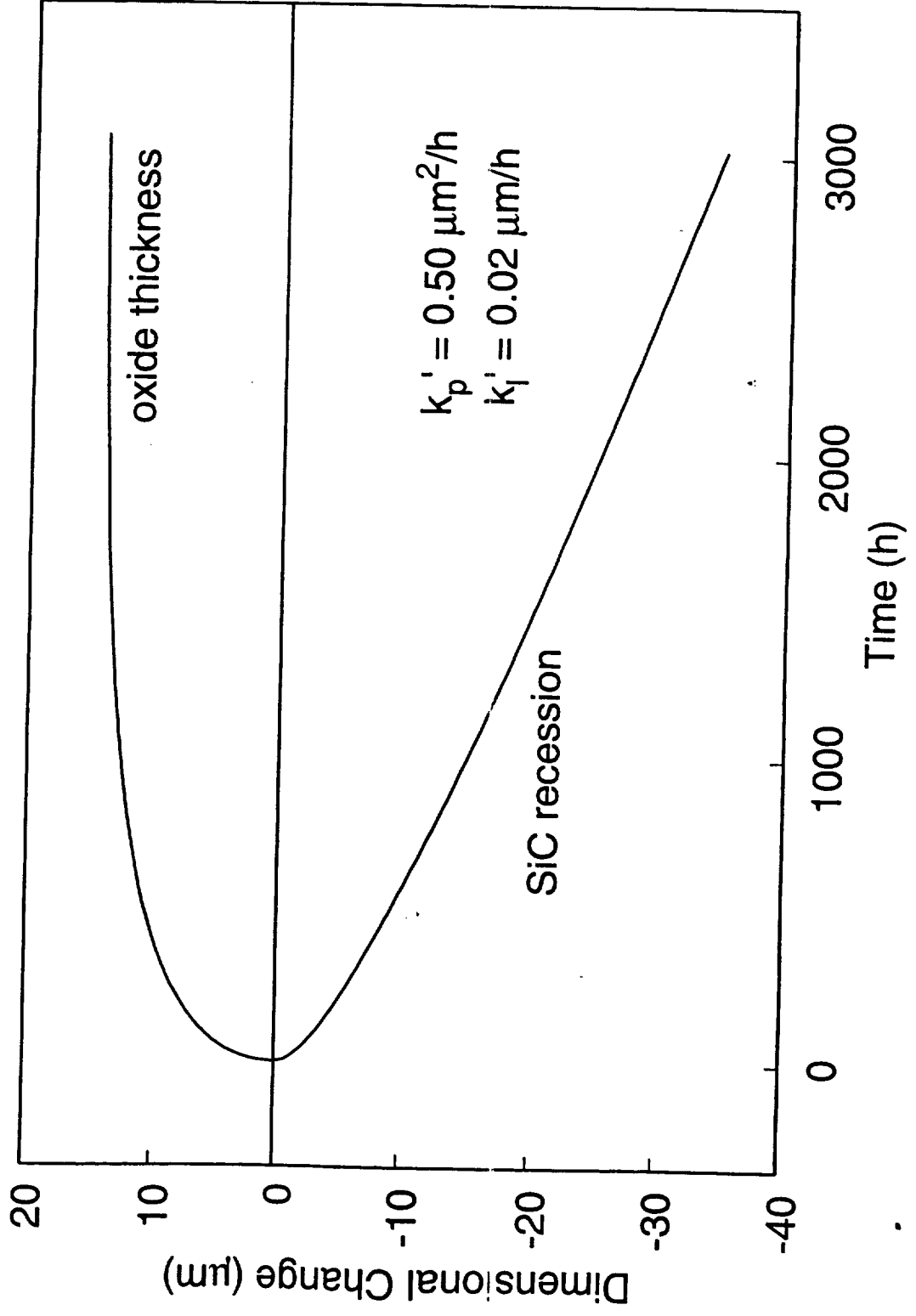
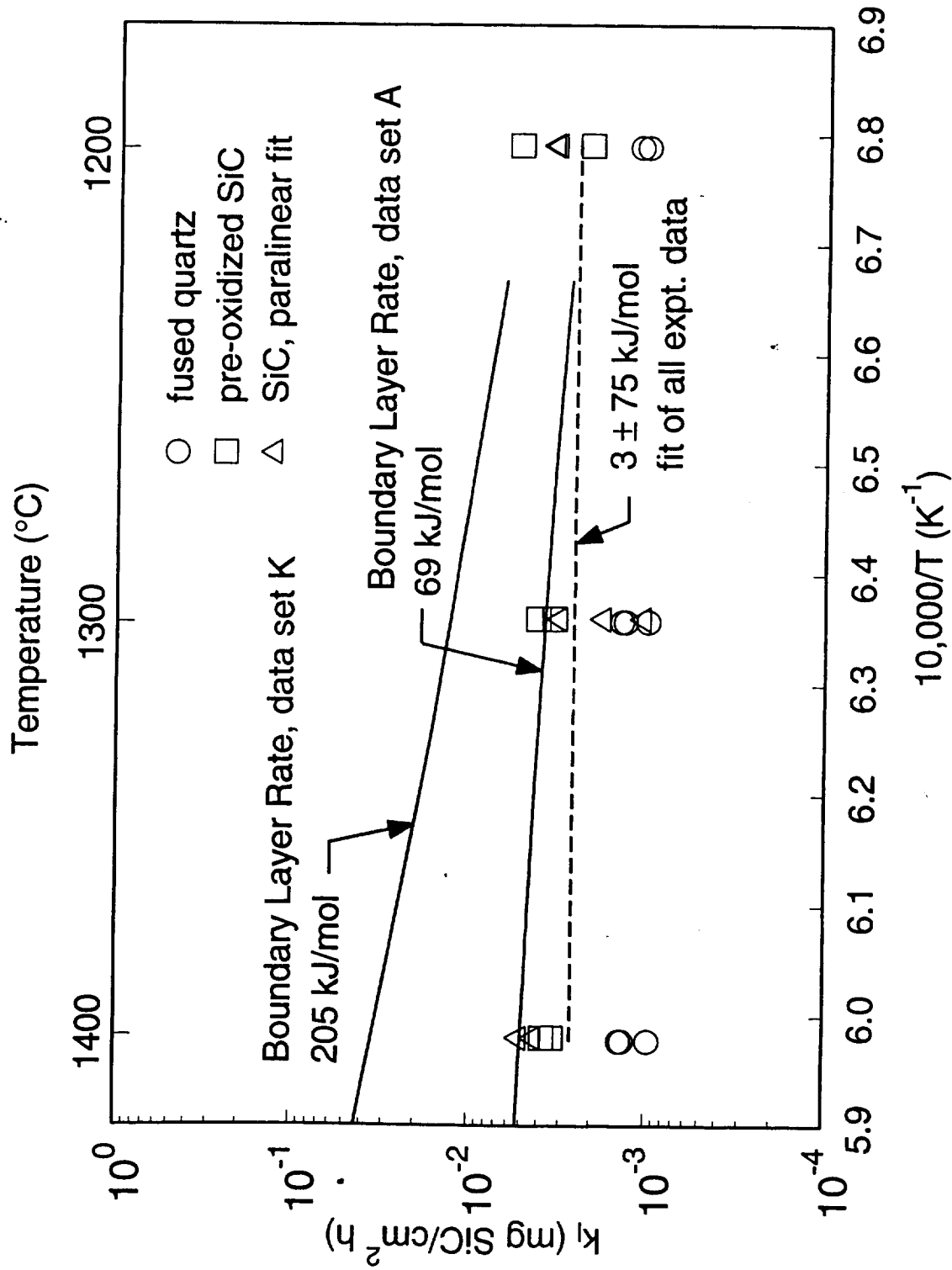


Fig 2-6

Linear Weight Loss Rates for SiC in 50% H₂O/50% O₂ at 4.4 cm/s



A Comparison of HPBR Data to Calculated Weight Loss

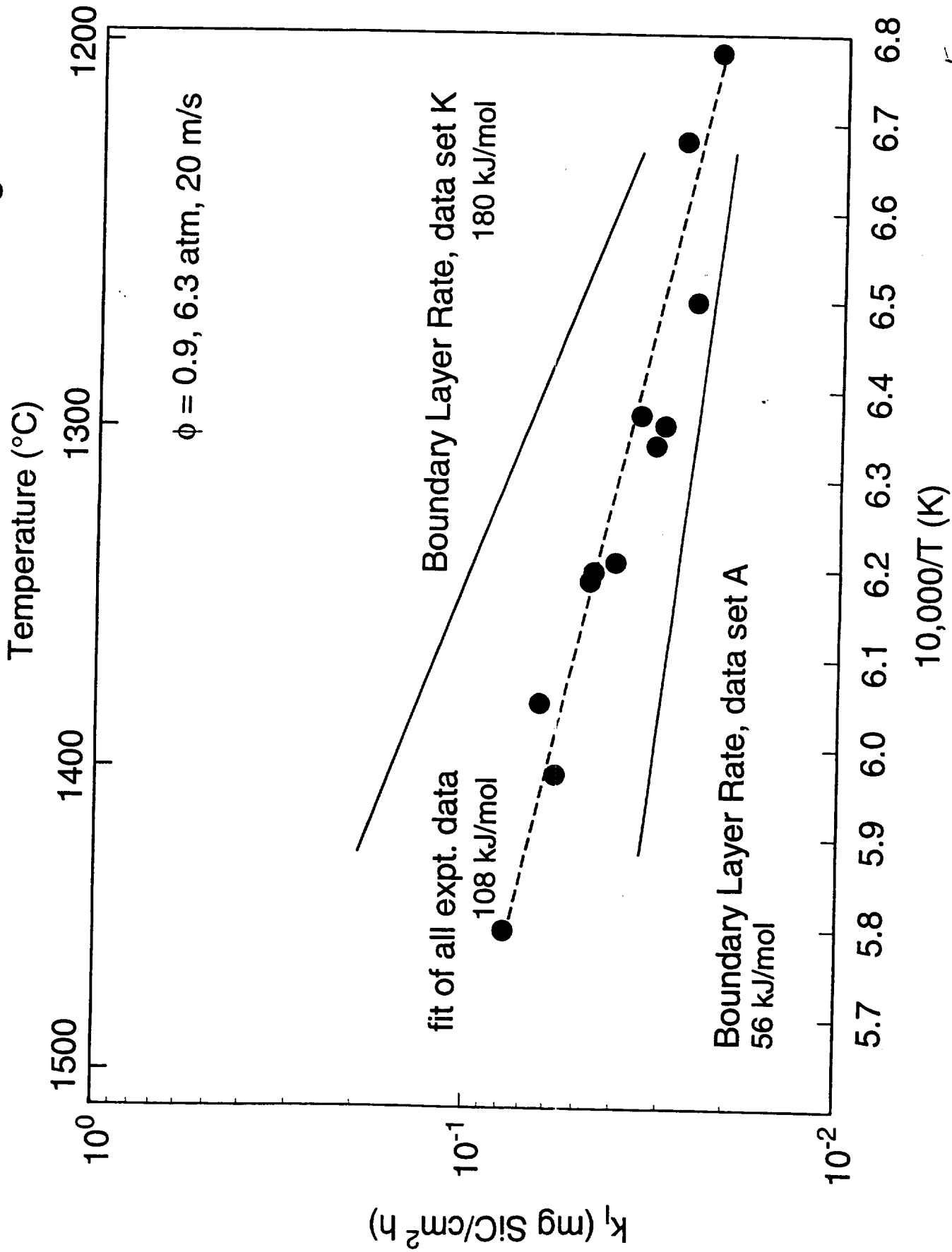


Fig 4

Linear Weight Loss Rates for SiC in Synthetic Fuel-Rich Conditions

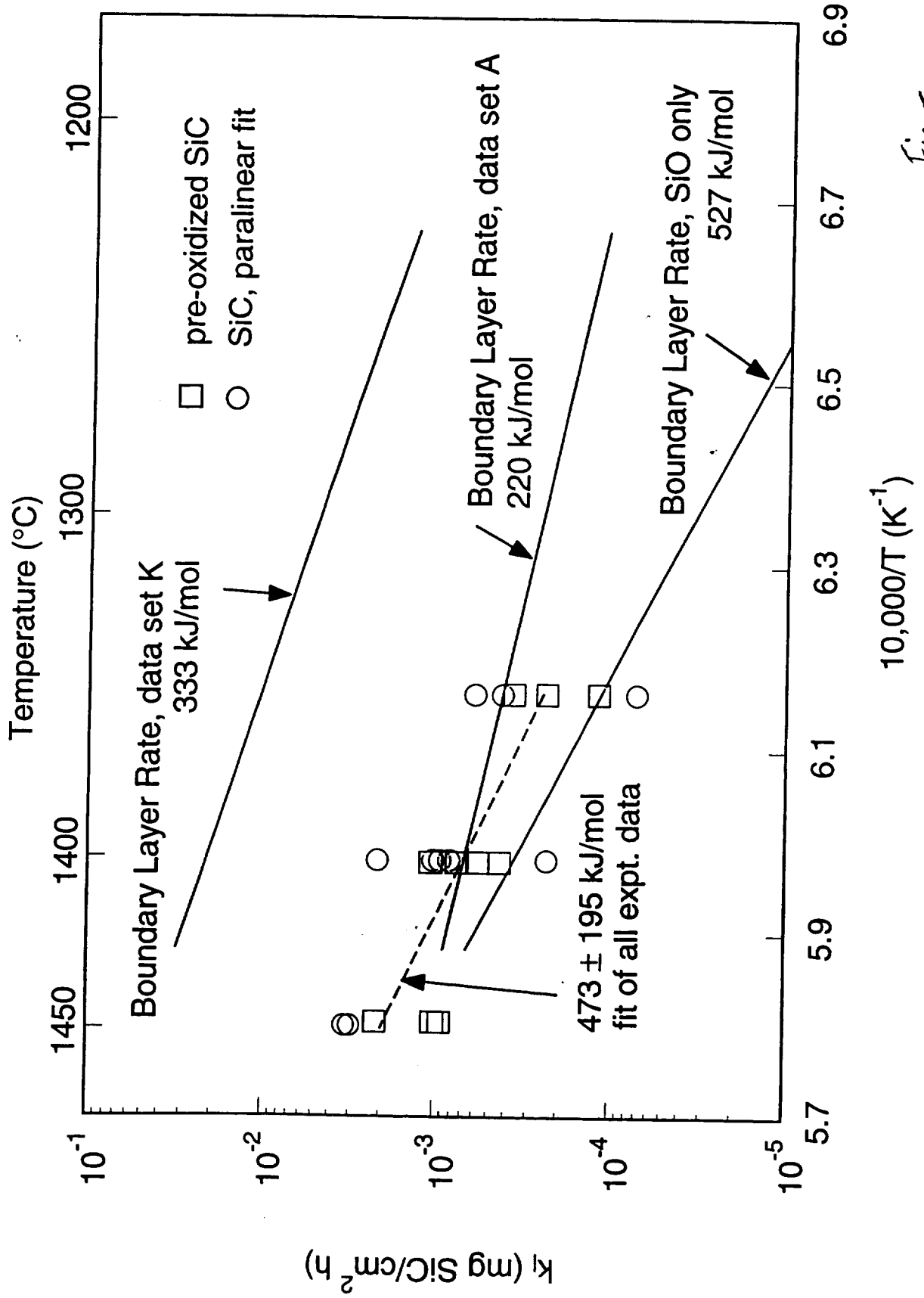
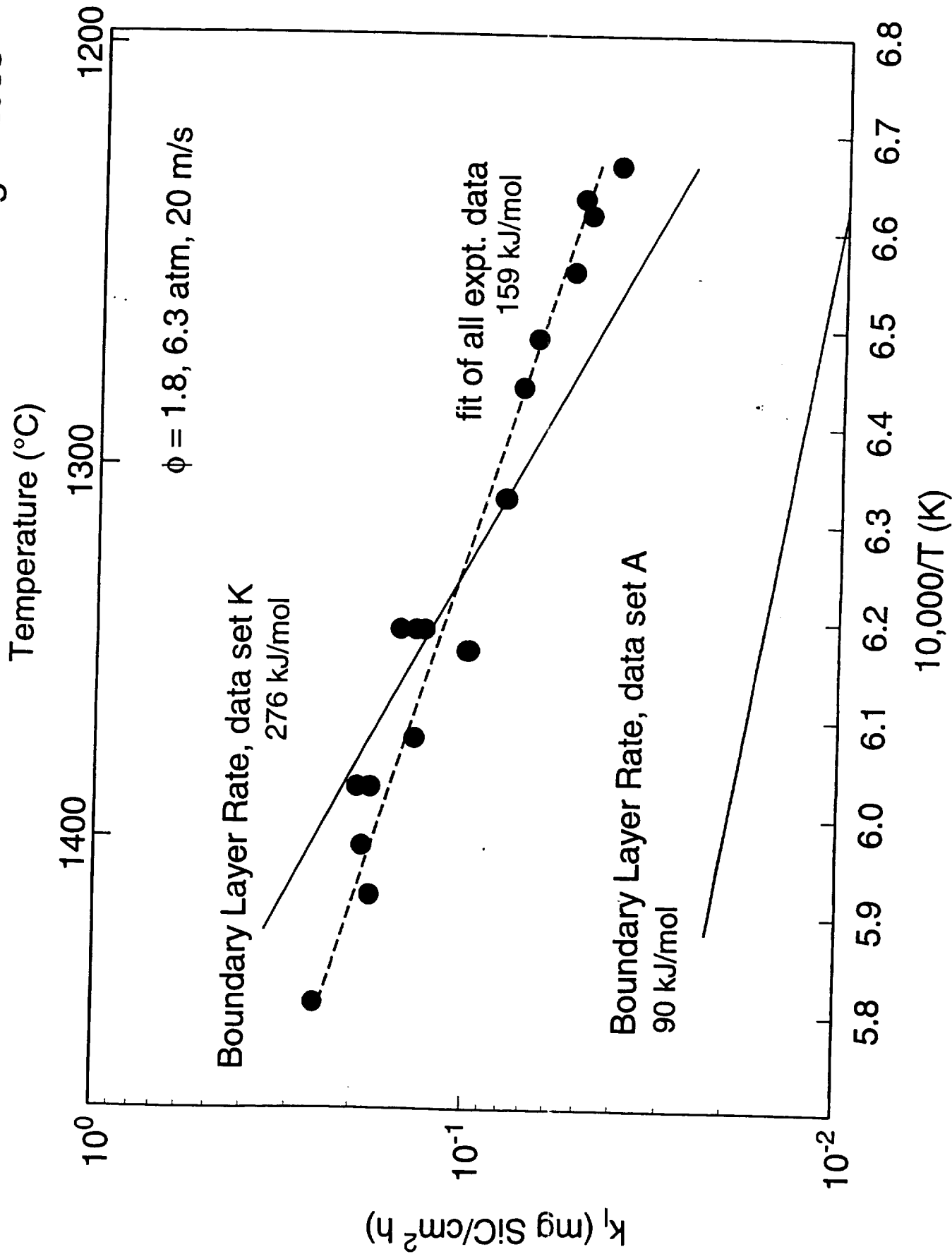


Fig. 5

A Comparison of HPBR Data to Calculated Weight Loss



Pressure dependence of SiO_xH_y at about 1650K

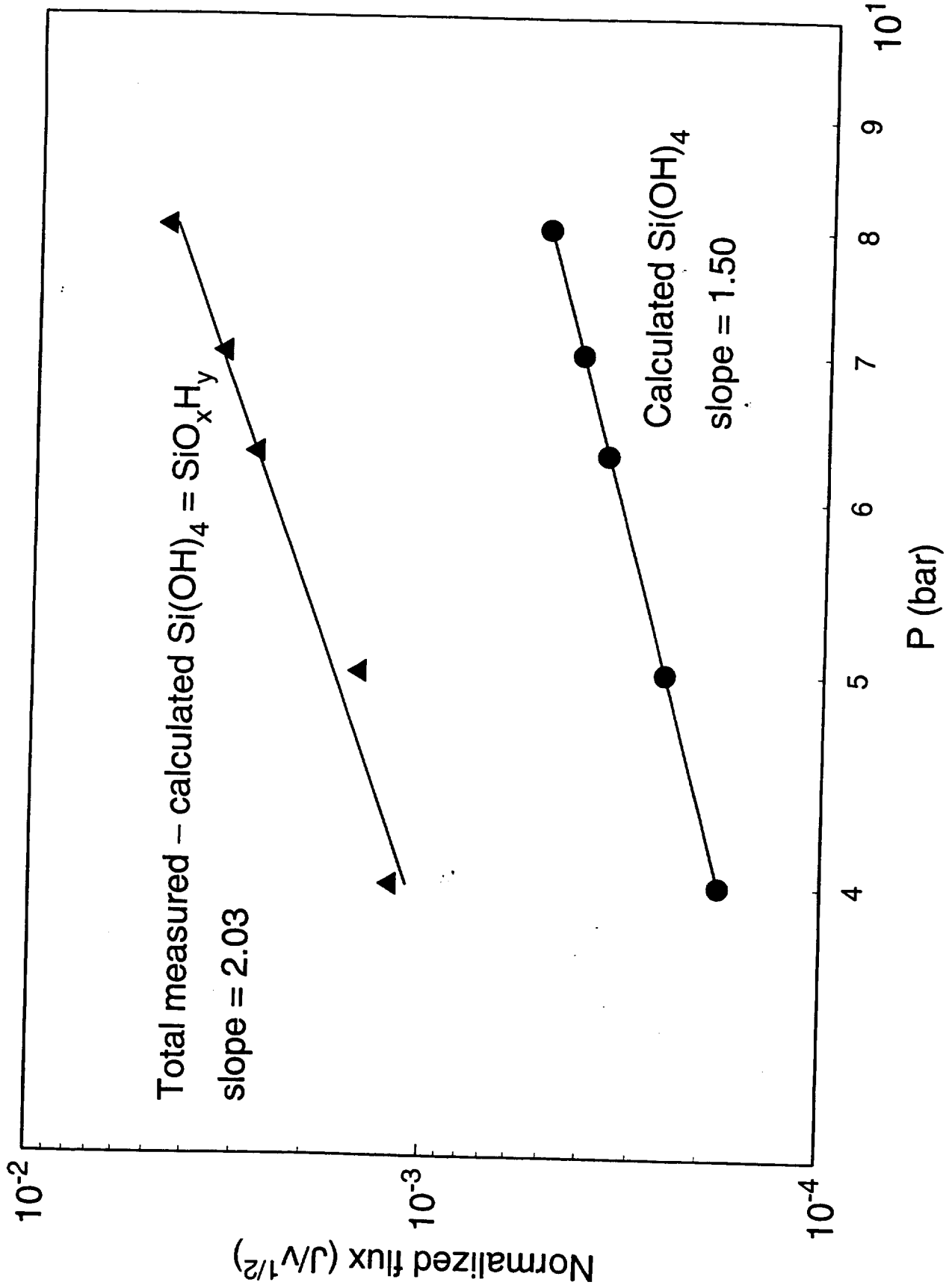


Fig. 7a

Temperature Dependence of SiO_xH_y

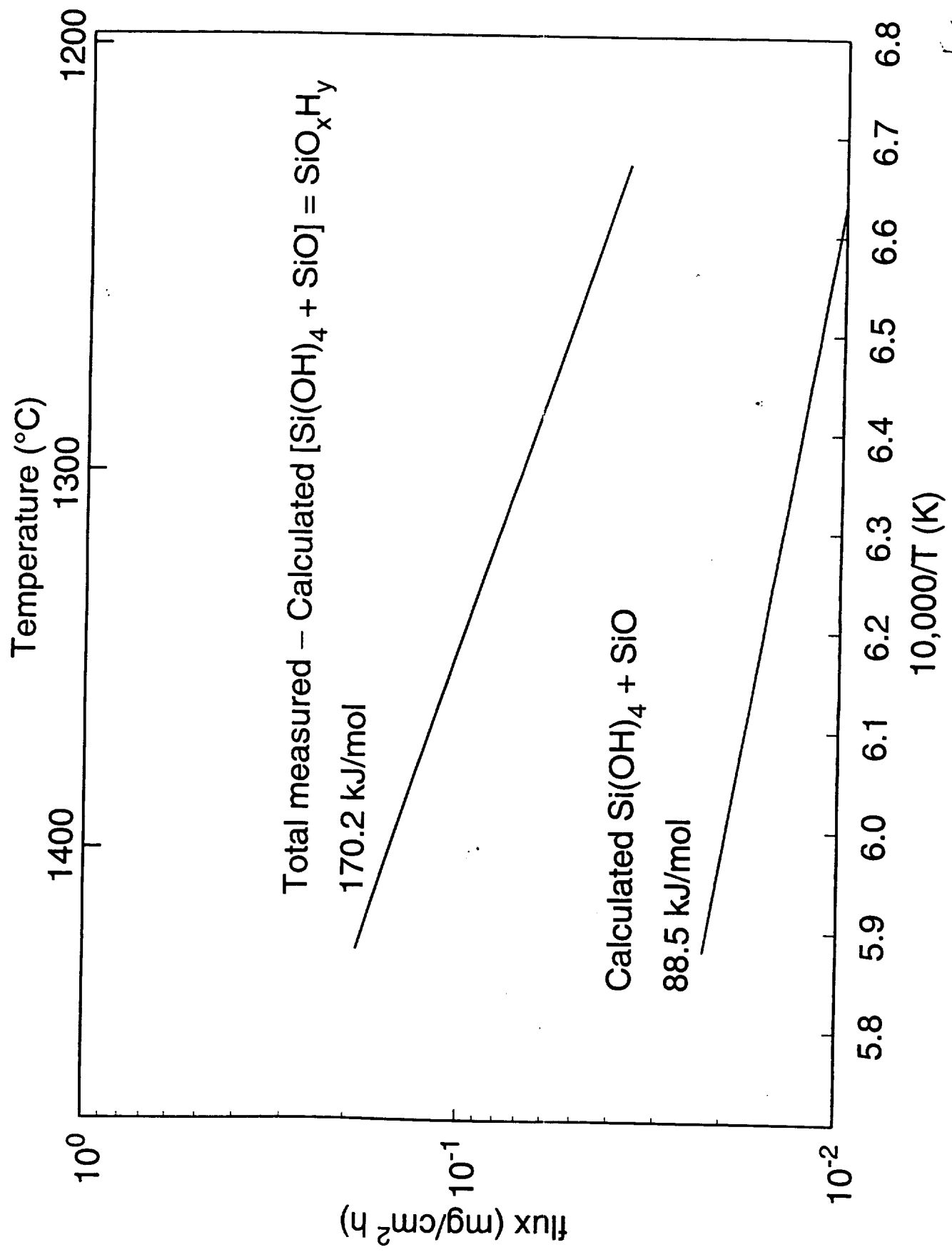


Fig. 76

Measured and Extrapolated Linear Weight Loss Rates for SiC

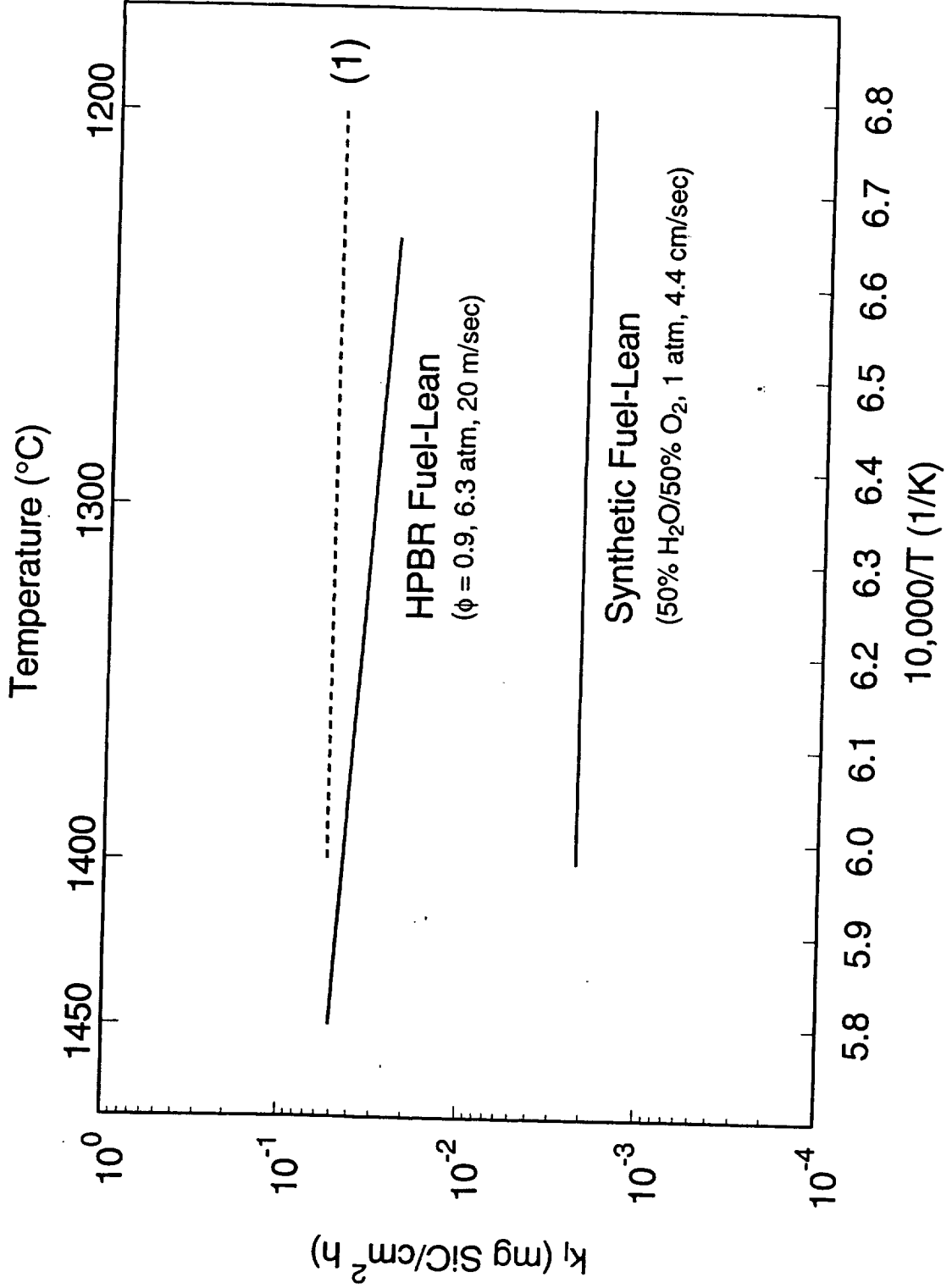


Fig 8a

Measured and Extrapolated Linear Weight Loss Rates for SiC

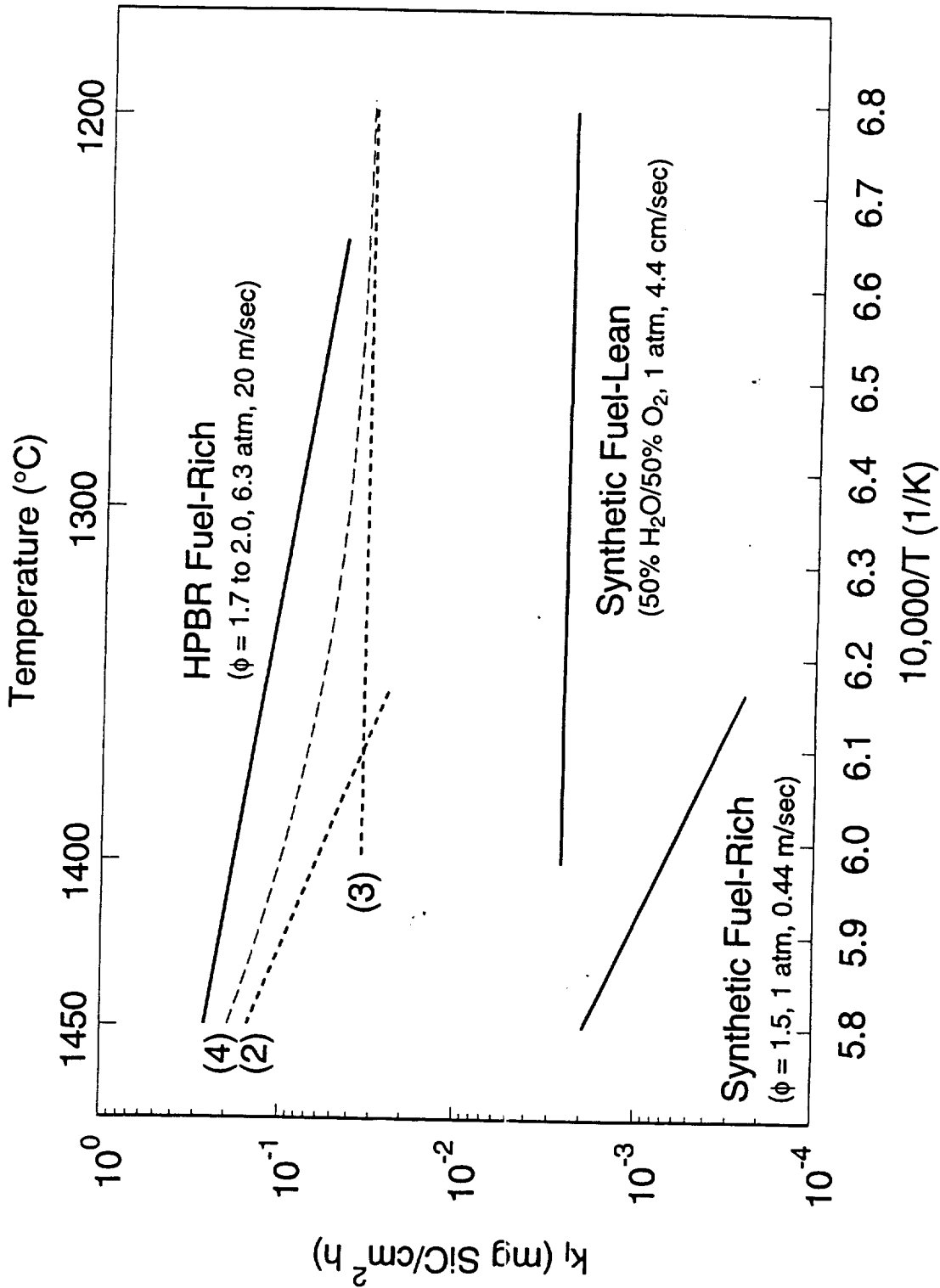


Fig 3b